PNAS
www.pnas.org

Supplementary Information for

A paradigm of thermal adaptation in vertebrates by tuning cold activation in TRPM8.

Shilong Yang, Xiancui Lu, Yunfei Wang, Lizhen Xu, Xiaoying Chen. Fan Yang, Ren Lai

Corresponding author: Ren Lai and Fan Yang
**Email:** rlai@mail.kiz.ac.cn or fanyanga@zju.edu.cn

**This PDF file includes:**
Supplementary text
Figures S1 to S10
Tables S1 to S6
Legends for Video S1
Legends for Datasets S1 to S5
SI References

**Other supplementary materials for this manuscript include the following:**
Video S1
Datasets S1 to S5



www.pnas.org/cgi/doi/10.1073/pnas.1922714117

**Supplementary Information Text**

## Materials and Methods

### Animals and sequencing data

All experiments involving animals conformed to the recommendations in the Guide for the Care and Use of Laboratory Animals of Kunming Institute of Zoology, Chinese Academy of Sciences. All experimental procedures were approved by the Institutional Animal Care and Use Committees at Kunming Institute of Zoology, Chinese Academy of Sciences (approval ID: SMKX-2018018). All possible efforts were made to reduce the sample size of mice and also to minimize mice suffering. *Aptenodytes forsteri trpm8* knock-in mice in the C57BL/6L background were commissioned by the Cyagen Biosciences, Inc. (Guangzhou, China). Sequencing data (PRJNA600306) of mice trigeminal ganglions have been deposited in the NCBI Sequence Read Archive (SRA).

### Cell transient transfection

HEK293 cells were cultured in Dulbecco's modified Eagle's medium with 10% fetal bovine serum and 1% penicillin/streptomycin, incubated at 37˚C with 5% $CO_2$. Cells were transfected with channel constructs and enhanced green fluorescent protein (eEGFP) plasmid by lipofectamine 2000 (Life Technologies, USA) following the manufacturer's protocol. Cells were later digested with 0.25% trypsin between one and two days after transfection. Patch clamp recordings were performed after the cells attached to the glass slide.

### Electrophysiology and compound perfusion

Whole-cell or inside-out patches were recorded with a HEKA EPC10 amplifier controlled by PatchMaster software (HEKA). Patch pipettes were pulled from borosilicate glass and fire-polished to resistance of ~3 MΩ. The solution containing 130 mM NaCl, 0.2 mM EDTA, and 3 mM Hepes (pH 7.2) were applied as both bath and pipette solutions. The membrane potential was held at 0 mV and the currents were elicited by two steps, 300 ms to 80 mV and followed by 300 ms to -80 mV. For single-channel recording, inside-out patches were recorded. The time for transfection was adjusted to 5 hours to increase the opportunity of obtaining a membrane with only one channel.
Gravity-driven system (RSC-200, Bio-Logic) was used to perfuse bath solution or menthol onto the cell or cell membrane. Bath and menthol solutions were flowed through separate tubes to minimize the mixing of the solutions. Patch pipette was placed in front of the perfusion tube outlet. Another perfusion tube was used to deliver precooled bath solution.

### Temperature control

To study the cold-driven activation of TRPM8, cells were first placed and recorded in 37˚C bath solution. Precooled bath solution was perfused through a separate perfusion tube. The pipette was placed about 1 mm from the solution output ports. To ensure the accuracy in monitoring of the local temperature, a TA-29 miniature bead thermistor (Harvard Apparatus) was placed right next to the pipette. The digital readout of thermistor was fed into an analog input of the patch clamp amplifier and recorded simultaneously with current signals.

### Gene synthesis and mutagenesis

The cDNA sequences of TRPM8 orthologues with their corresponding NCBI code are: *Loxodonta africana* (African savanna elephant) *trpm8* (100669499), *Camelus bactrianus* (Bactrian camel) *trpm8* (105063570), *Homo sapiens trpm8* (79054), *Mus musculus trpm8* (171382), *Jaculus jaculus* (lesser Egyptian jerboa) *trpm8* (101612379), *Bos mutus* (wild yak) *trpm8* (102279011), *Pantholops hodgsonii* (chiru) *trpm8* (102329712) and *Aptenodytes forsteri* (emperor penguin) *trpm8* (103903828) orthologues were synthesized by Tsingke (Beijing, China) based on the predicted gene sequence and subcloned into the pCDNA3.1 vector. All TRPM8 point mutants were constructed using Fast Mutagenesis Kit V2, (SBS Genetech,Co., Ltd, China) following the manufacturer's instruction.

### Site-directed fluorescence recordings

L-ANAP methyl ester was purchased from AsisChem. pANAP vector was purchased from Addgene. ANAP was incorporated into TRPM8_LA protein by introducing a TAG amber stop codon mutation. During transfection, 1 μg pANAP vector was co-transfected with 3 μg plasmid of TRPM8 mutant

and 1 μg eEGFP plasmid. 20 μM ANAP directly mixed into the culture medium. HEK293 cells expressing ANAP-incorporated TRPM8_LA channels were digested after 24 hours transfection. Electrophysiological recordings were performed until cells attached to the glass slide.
ANAP fluorescence images of HEK-293 cells were acquired with an Olympus IX71 microscope with Hamamatsu R2 charge-coupled device camera controlled by the MetaFluor Software (Molecular Devices). ANAP spectrum was excited by single-wavelength laser (Cobolt Zouk) with 330-385 nm excitation filter. The recorded emission spectra treated by a long-pass emission filter (greater than 420 nm) were analyzed by spectrometer (Princeton Instruments) and were measured by fitting to the skewed Gauss equation.

**Calculation of ΔH and ΔS**
To calculate the change of enthalpic (ΔH) and entropic (ΔS) due to the temperature-driven transition of TRPM8, we constructed Van't Hoff plots and fitted them to the equation ln Keq = -ΔH/RT + ΔS/R whereby R represents the gas constant, T represents the temperature in Kelvin, Keq represents the equilibrium constant measured from the cold-driven TRPM8 open probability, Keq = Po/(1-Po). The TRPM8 open probability induced by menthol at saturated concentration was served as the maximum open probability.

**Calculation of the hydrophobicity of TRPM8 pore domain**
The amino acid sequences of TRPM8 pore region from different species were aligned. The expected hydrophobic scales of natural amino acids were cited from (1) and (2). The hydrophobicity value of non-conserved residues was accumulated and served as the estimated hydrophobicity of TRPM8 pore domain.

**Molecular modeling**
To model the closed state and the cold-induced open state of TRPM8, membrane-symmetry-loop modeling was performed using the Rosetta molecular modeling suite version 2016.20 (3). The cryo-EM structure of TRPM2 in closed state (PDB: 6drk) was used as the template. The selectivity filter was modeled *de novo* with the kinematic closure (KIC) loop modeling protocol (4, 5). We generated 10,000 to 20,000 models in each round. Among these models, the top 10 models ranked by energy were used as input for the next round of modeling. After four rounds of KIC loop modeling, the top ten models converged well. The model with the lowest energy was finally selected as the closed state model. To model the cold-induced open state, the models generated in the first round were filtered by the SASA value at sites 925 943 947 of TRPM8_LA. Only the models that the SASA values increased larger than 10 $Å^2$ compared with the closed state were allowed to pass. Among these filtered models, the top 10 models ranked by energy were selected and input for next round of loop modeling. After several rounds of KIC loop modeling, the top ten models converged well. The model with the lowest energy was finally selected as the cold-driven open model of TRPM8. The closed state and the cold-induced open stated models were further refined by the relax application within the Rosetta suite, where energy minimization of side-chain of all residues in TRPM8 models was executed (6). The side-chain conformations of ANAP within the TRPM8 models were modeled according to procedures as previously described (7).
SASA of each residue in TRPM8_LA models was measured by RosettaScripts within the Rosetta suite (8). Command lines employed in Rosetta to perform the modeling processes, the SASA measurements and filtering are appended.
Pore radius of TRPM8_LA models was calculated by the HOLE program version 2.0 (9).
All the molecular graphics of TRPM8 models were rendered by UCSF Chimera software version 1.12 (10).

**RNA-sequencing**
Total RNA was extracted from the trigeminal ganglions of both wild type and AF mice by using RNeasy Mini Kit (Qiagen). The sequencing libraries were constructed and were subjected to DSN normalization (New England Biolabs, Inc.). According to the manufacturer's protocol, each library was sequenced on a hiseq X ten, generating 150-bp paired-end reads (NextOmics, Inc.). Reads alignment was carried out by using the splice-aware tool Tophat2 (v2.0.5). Read counts of per

feature (genes or exons) were analyzed by StringTie (v1.3.0). To indicate differentially expressed genes, the count data were further analyzed using DESeq2 (v1.01.1) at FDR 5%.

**Immunoblotting**

Trigeminal ganglia neurons isolated from mice were washed in Phosphate buffer saline (PBS) and homogenized using a T10 basic ULTRA-Turrax (IKA) in RIPA lysis buffer (R0278, Sigma) with protease inhibitors (P8340, Sigma) and phosphatase inhibitors (P5726, Sigma). Lysis solutions were centrifuged at 4°C for 15 minutes at 12,000g and the supernatants were collected. The protein concentrations in the supernatants were determined using the BCA assay kit (23225, Thermo). The protein samples were boiled for 5 minutes with 5× loading buffer (BL502A, Biosharp) and then separated by 12% SDS-PAGE. The protein bands were transferred to PVDF membranes (ISEQ00010, Millipore). The PDVF membranes were blocked by 5% BSA dissolved in TBST solution containing 0.1% Tween-20 for 1 hour at room temperature and incubated with the primary antibodies (Rabbit TRPM8 Antibody, Affinity #DF7966 and Mouse β-Actin Antibody, SantaCruz sc-69879) overnight at 4°C. Then the PDVF membranes were washed with TBST three times and incubated with the secondary antibodies (peroxidase-labeled anti-rabbit antibody, Affinity #DF7074 or peroxidase-labeled anti-mouse antibody, Affinity #DF7076) for 1 hour at room temperature. After incubation, the PDVF membranes were washed again three times and exposed to chemiluminescent reagents. The images were acquired with an ImageQuant LAS 4000 instrument (GE HealthCare).

**Calcium fluorescence imaging**

Mouse DRG neurons were acutely dissociated and maintained in a short-term primary culture according to procedures as previously described (11). DRG neurons were loaded with Fluo-4 AM in Ringer's solution (140 mM NaCl, 5 mM KCl, 2 mM $MgCl_2$, 10 mM glucose, 2 mM $CaCl_2$ and 10 mM HEPES, pH 7.4) for 40-60 minutes. Calcium fluorescence images of the DRG neurons were acquired with an Olympus IX71 microscope with Hamamatsu R2 charge-coupled device camera controlled by the MetaFluor Software (Molecular Devices). 1 mM Ionomycin was used as the positive control. Fluo-4 was excited by a LED light source (X-Cite 120LED, Lumen Dynamics) with a 500/20 nm excitation filter and a 535/30 nm emission filter.

**Immunofluorescence**

Trigeminal ganglions of mice were first fixed using 10% formalin and then dehydrated with an increasing concentration of alcohol. The tissues were then embedded in paraffin and sectioned to a thickness of 5 μm using a histocut (Leica). After dewaxing and antigen repairing, the tissue sections were blocked by 3% BSA and incubated with the primary antibody (Rabbit TRPM8 Antibody, Proteintech #12813-1-AP) overnight at 4˚C. The sections were washed in PBS again and incubated with the secondary antibody (CY3-labeled anti-rabbit antibody, Servicebio #GB21303) for 50 minutes at room temperature in the dark. The sections were then repeatedly washed with PBS and incubated with 4',6-diamidino-2-phenylindole (DAPI) for 10 minutes at room temperature in the dark. Afterwards, the sections were washed in PBS again and blocked by mounting medium for preventing fluorescence quenching. Finally, the fluorescence images of sections were acquired with a confocal laser scanning microscope (Olympus, FV1000, Japan).

**Animal behaviors assay**

For the two-temperature choice assay, mice were individually confined in two adjacent Plexiglas chambers and allowed to move freely between these chambers. The plate temperature of one chamber was held at 30˚C and the other ranged from 6 to 50˚C. The time spent of each mouse on the two chambers was recorded every 3 minutes.

For the temperature preference assay, mice were individually confined in a Plexiglas chamber on a gradient cooling plate ranging from 4°C to 50°C. The movements of mice were recorded by a thermal imaging camera (FLIR T640). The time spent on plate at different temperature was analyzed by the FLIR tools.

**Statistics**

All experiments were independently repeated for at least three times. All statistical data are given as mean ± s.e.m.. Two-sided Student's t-test was applied to examine the statistical significance. ** indicates p <0.05, and *** indicates p <0.001 respectively.

**Commands in Rosetta to perform loop modeling**

```
/home/fan/rosetta_2016.20/main/source/bin/loopmodel.mpi.linuxgccrelease \
-in:path:database /home/fan/rosetta_2016.20/main/database \
-score:weights membrane_highres_Menv_smooth.wts \
-in:file:fullatom \
-membrane:normal_cycles 100 \
-membrane:normal_mag 15 \
-membrane:center_search \
-ignore_unrecognized_res \
-constraints true \
-constraints:cst_file
/home/fan/Rosetta/Project_LA_TRPM8/SS_C197C208_cen.cst \
-symmetry:symmetry_definition
/home/fan/Rosetta/Project_LA_TRPM8/4D_LA_M8TM.r.symm \
-symmetry:initialize_rigid_body_dofs \
-in:file:spanfile /###.span \
-in:file:s /###.pdb \
-loops:loop_file /###.loop \
-loops:remodel perturb_kic \
-loops:refine refine_kic \
-loops:relax no \
-loops:strict_loops \
-loops:build_attempts 20 \
-relax:bb_move false \
-max_inner_cycles 30 \
-nstruct 10000 \
-out:file:silent /###.silent \
-out:file:silent_struct_type binary \
-overwrite
```

**Commands in Rosetta to perform SASA calculation and filtering**

```
/home/fan/rosetta_2016.20/main/source/bin/rosetta_scripts.linuxgccrelease \
-database /home/fan/rosetta_2016.20/main/database
-membrane:normal_cycles 100
-membrane:normal_mag 15
-membrane:center_search
-in:file:spanfile /###.span
-score:weights membrane_highres_Menv_smooth.wts
-parser:protocol /###.xml
-symmetry:symmetry_definition /###.symm
-symmetry:initialize_rigid_body_dofs
-ignore_unrecognized_res
-in:file:silent_struct_type binary
-in:file:silent /###.out
-nstruct 1
-out:file:silent /###.silent
-out:file:silent_struct_type binary
-overwrite
```

**Rosetta scripts to perform SASA calculation and filtering**

```
<ROSETTASCRIPTS>
<RESIDUE_SELECTORS>
```

```
<Not name="G925_unselected">
<Index resnums=925/>
</Not>
<Not name="L943_unselected">
<Index resnums=943/>
</Not>
<Not name="L947_unselected">
<Index resnums=947/>
</Not>
</RESIDUE_SELECTORS>
<TASKOPERATIONS>
<OperateOnResidueSubset name="G925_only"
selector="G925_unselected" >
<PreventRepackingRLT/>
</OperateOnResidueSubset>
<OperateOnResidueSubset name=L943_only"
selector="L943_unselected" >
<PreventRepackingRLT/>
</OperateOnResidueSubset>
<OperateOnResidueSubset name="L947_only"
selector="L947_unselected" >
<PreventRepackingRLT/>
</OperateOnResidueSubset>
<PreventRepackingRLT/>
</OperateOnResidueSubset>
</TASKOPERATIONS>
<SCOREFXNS>
</SCOREFXNS>
<FILTERS>
<TotalSasa name=G925_sasa threshold=10
task_operations=G925_only report_per_residue_sasa=1/>
<TotalSasa name=L943_sasa threshold=10
task_operations=L943_only report_per_residue_sasa=1/>
<TotalSasa name=L947_sasa threshold=10
task_operations=L947_only report_per_residue_sasa=1/>
</FILTERS>
<MOVERS>
</MOVERS>
<PROTOCOLS>
<Add filter=G925_sasa/>
<Add filter=L943_sasa/>
<Add filter=L947_sasa/>
</PROTOCOLS>
</ROSETTASCRIPTS>
```

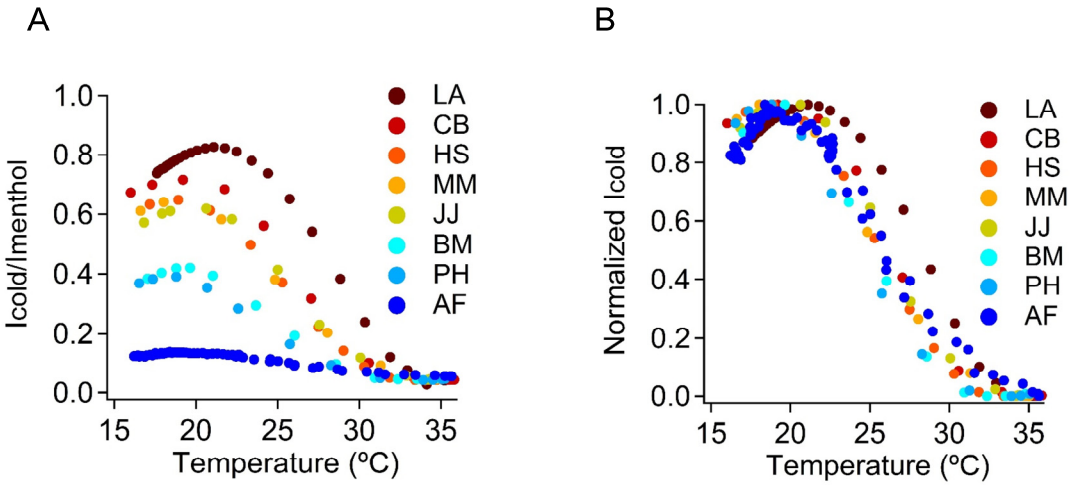


**Fig. S1.** Temperature response profile of each TRPM8 orthologue. (A, B) Representative temperature-driven activation of TRPM8 orthologues. The cold-activated currents were normalized to saturated menthol-induced activation (A) or the maximum cold-activated currents (B).

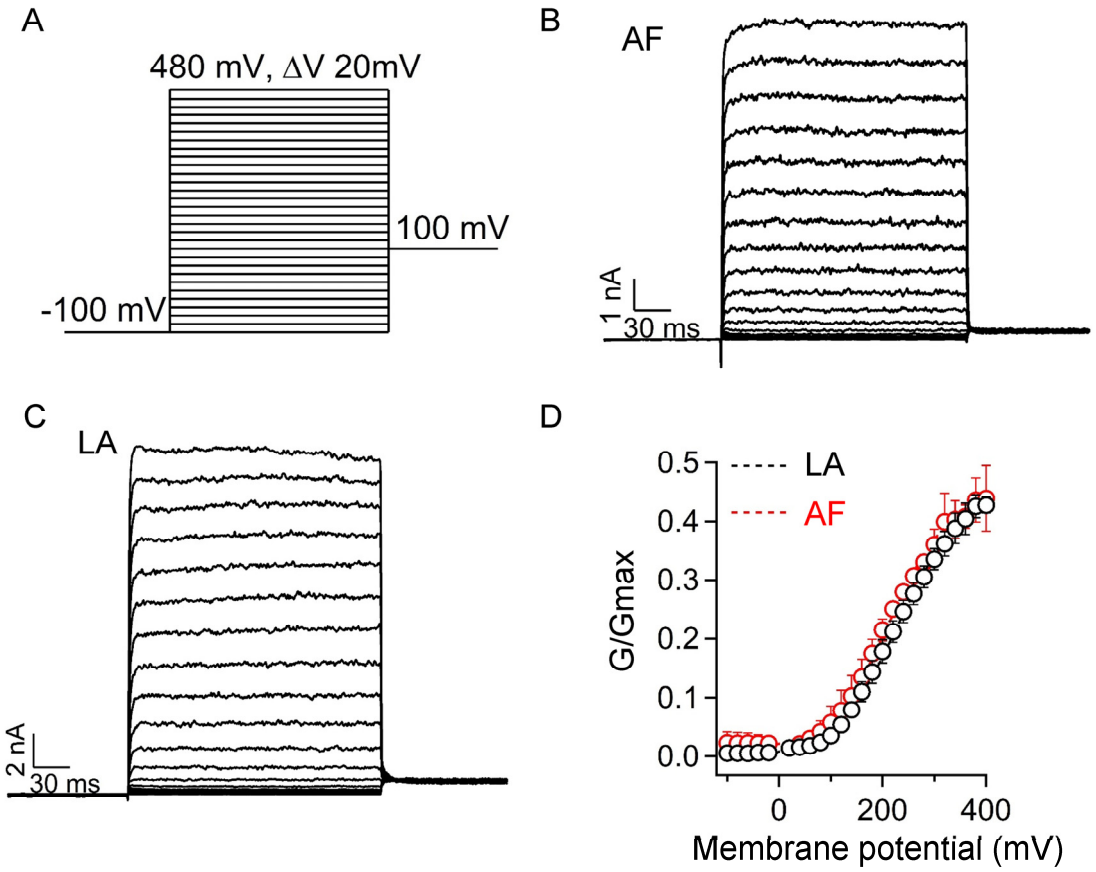


**Fig. S2.** Voltage dependence of TRPM8_AF and TRPM8_LA. (A) The voltage protocol for the voltage-induced activation recording. (B, C) Representative voltage-gated currents of (B) TRPM8_AF and (C) TRPM8_LA were recorded at 32°C. (D) The conductance-voltage relationships of TRPM8_AF and TRPM8_LA (mean ± s.e.m., n=3).

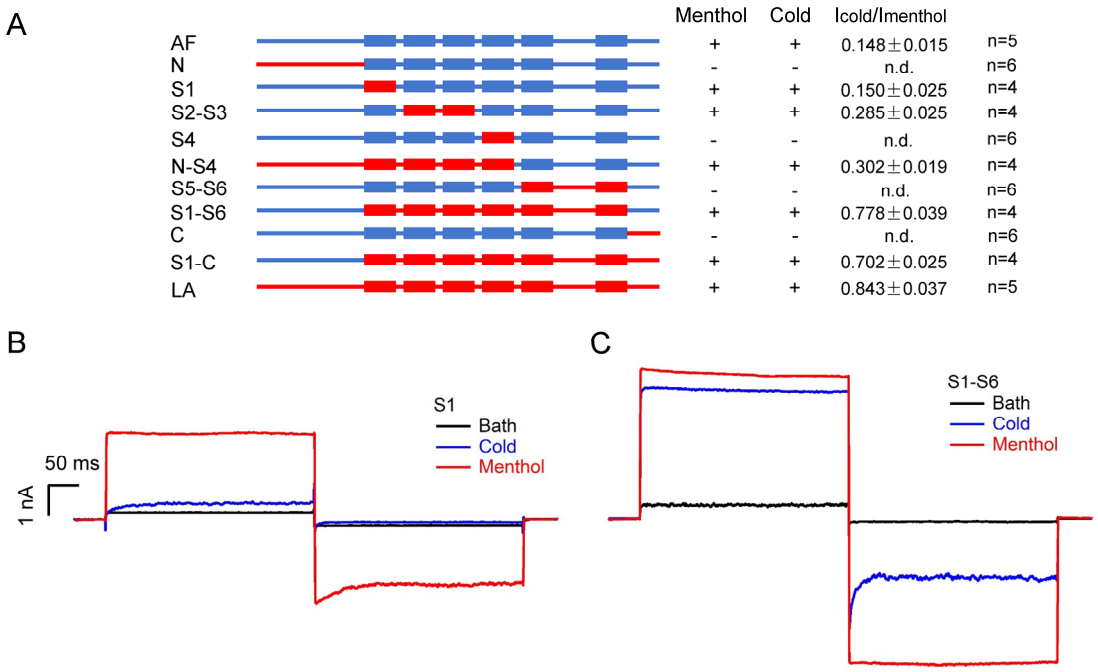


**Fig. S3.** The chimeras containing the TRPM8_LA PD alter cold activation of TRPM8_AF. (A) Responsiveness to cold and menthol by channel mutants between TRPM8_AF (in blue) and TRPM8_LA (in red). (B, C) Representative whole-cell current responses of (B) S1 and (C) S1-S6 chimeric channels to cold and 1 mM menthol.

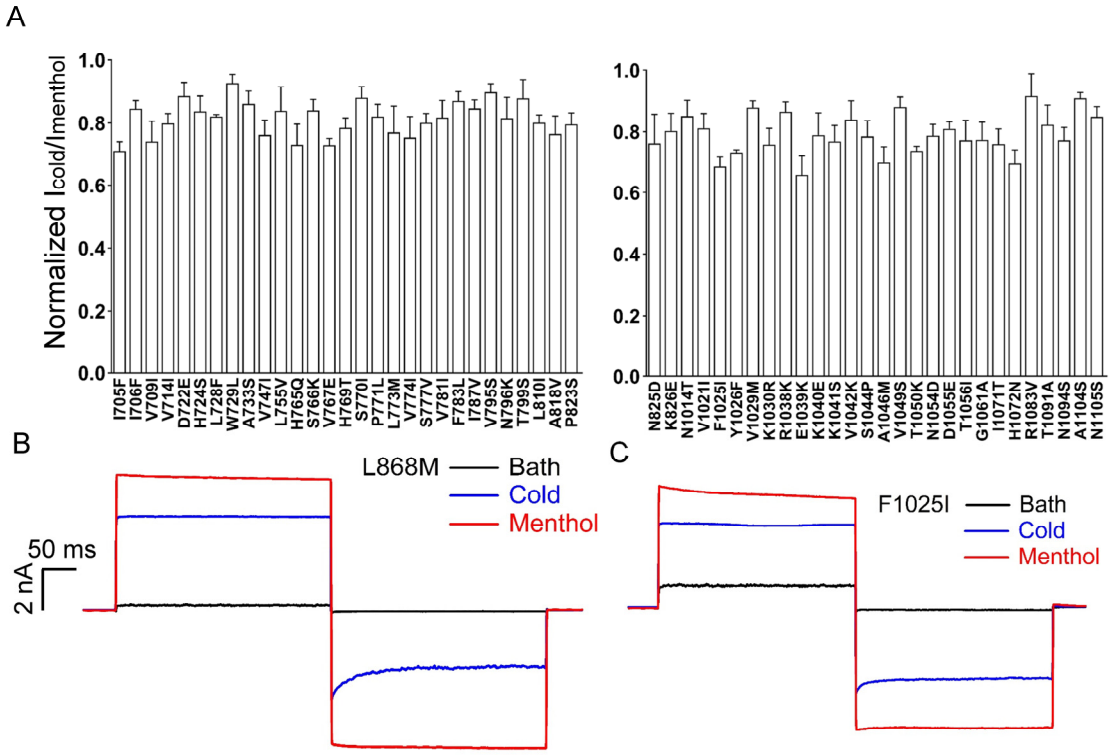


**Fig. S4.** The cold activation of TRPM8_LA point mutants. (A) Cold-activated currents of TRPM8_LA mutants were normalized to saturated menthol-induced currents (mean ± s.e.m., n=3). (B, C) Representative currents of the channel mutants (B) L868M and (C) F1025I activated by cold and 1 mM menthol.

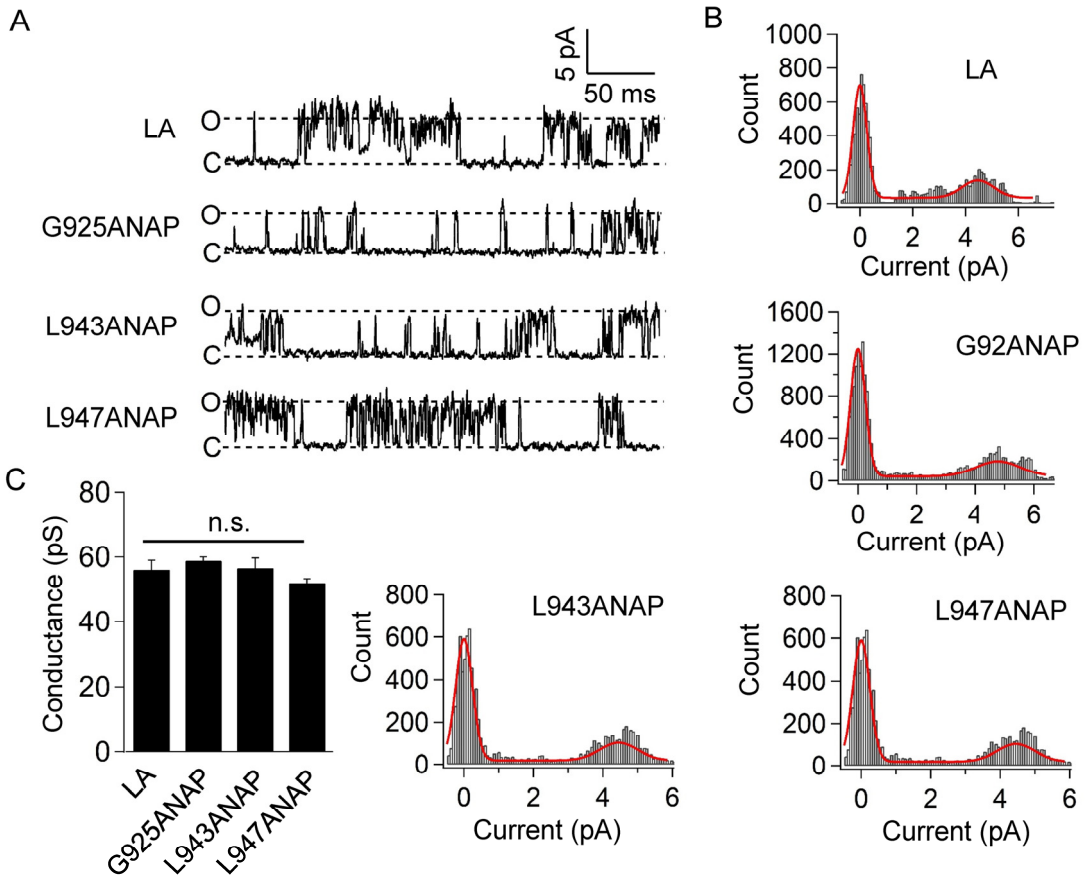


**Fig. S5.** ANAP-incorporated channels exhibit normal single conductance. (A) The single-channel events of wild-type TRPM8_LA and ANAP-incorporated TRPM8_LA activated by cold. (B) All-point histogram of the representative single-channel traces. The histogram was fitted to a double gauss function (in red). (C) Single-channel conductance of TRPM8_LA and ANAP-incorporated TRPM8_LA channels (mean ± s.e.m., n=3).

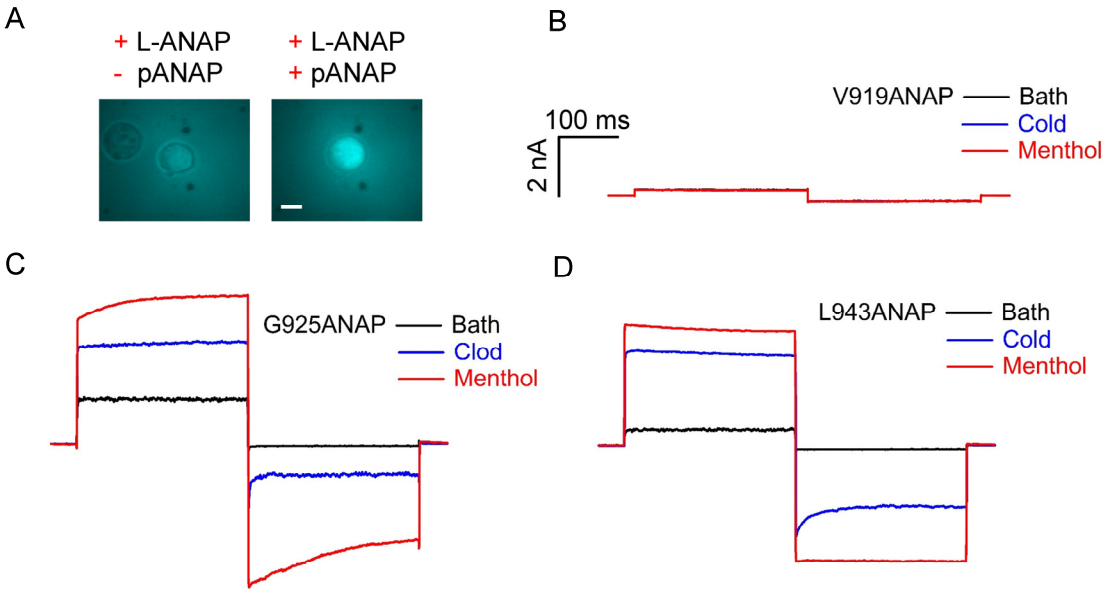


**Fig.** S6. The cold activation of ANAP-incorporated TRPM8_LA. (A) Expressing of ANAP-incorporated TRPM8_LA (at site 919) in HEK293 cells in the presence or absence of pANAP vector. Scale bar, 10 μm. (B, C, D) Representative whole-cell current response of (B) V919ANAP, (C) G925ANAP and (D) L943ANAP activated by cold and 1 mM menthol.

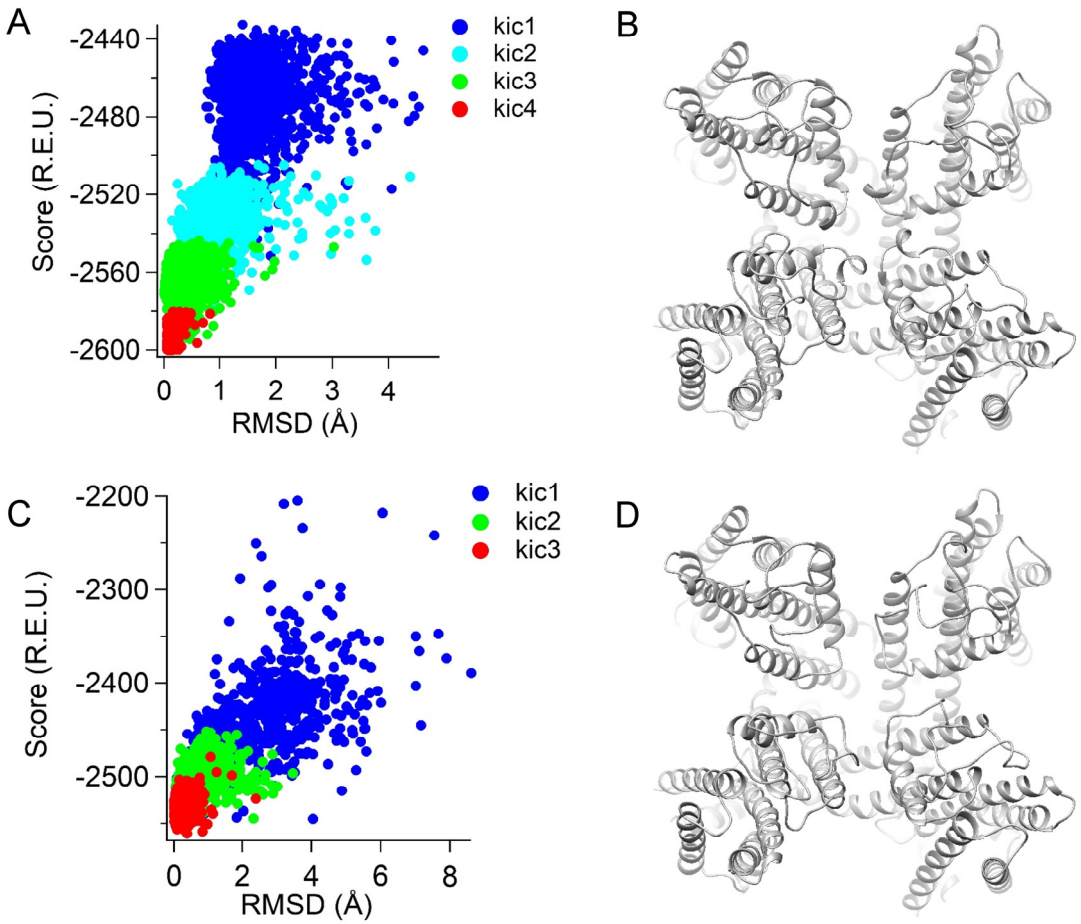


**Fig. S7.** Modeling of the TRPM8_LA channel in the closed and cold-activated states. (A) The TRPM8_LA models in closed state after four rounds of KIC loop modeling exhibited a funnel-shaped distribution of total energy calculated by Rosetta (R.E.U., Rosetta energy unit). (B) The TRPM8_LA model with the lowest energy in the closed state. (C) Three rounds of KIC loop modeling for calculating the TRPM8_LA model in the cold-activated state. (D) The TRPM8_LA model with the lowest energy in the cold-activated state.

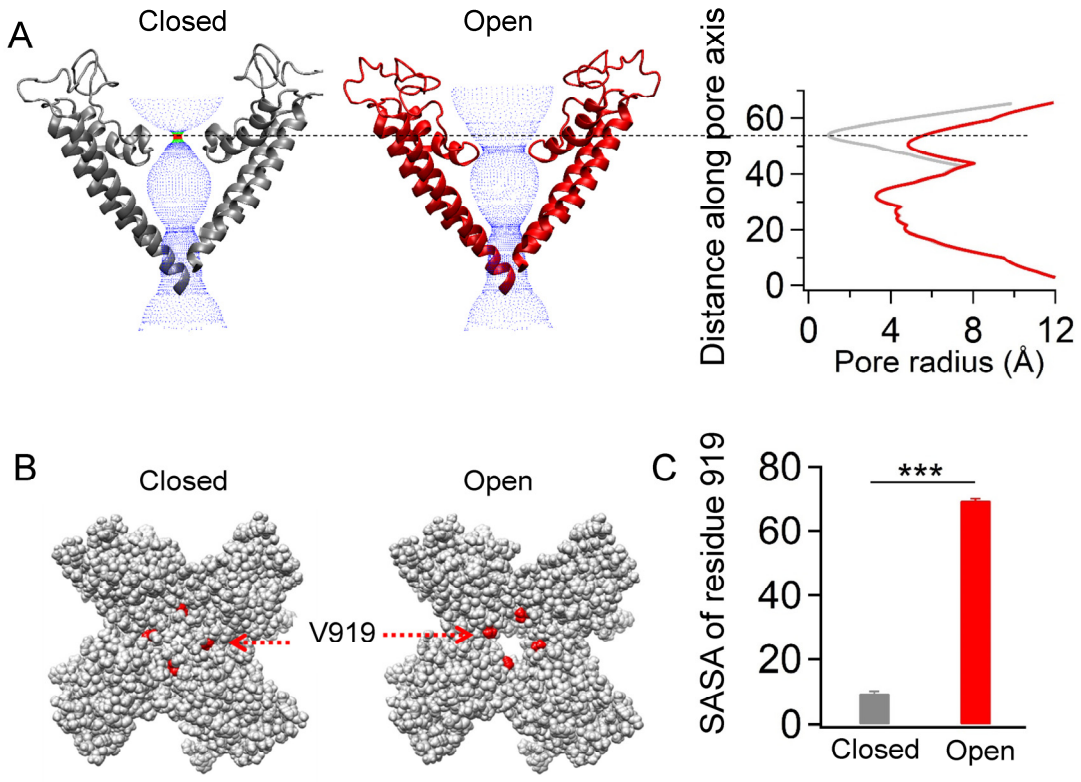


**Fig. S8.** Predicted conformational changes of PD during TRPM8_LA cold activation. (A) Distribution of pore radii in the TRPM8_LA structure models in closed state and cold-activated state. Pore radii were calculated by the HOLE program. (B) The 919 site (red) was mapped on TRPM8_LA structure models in the closed and cold-activated states, respectively. (C) SASA of residue V919 was calculated in the closed and cold-activated states (mean ± s.e.m., ***P<0.001, n=4).

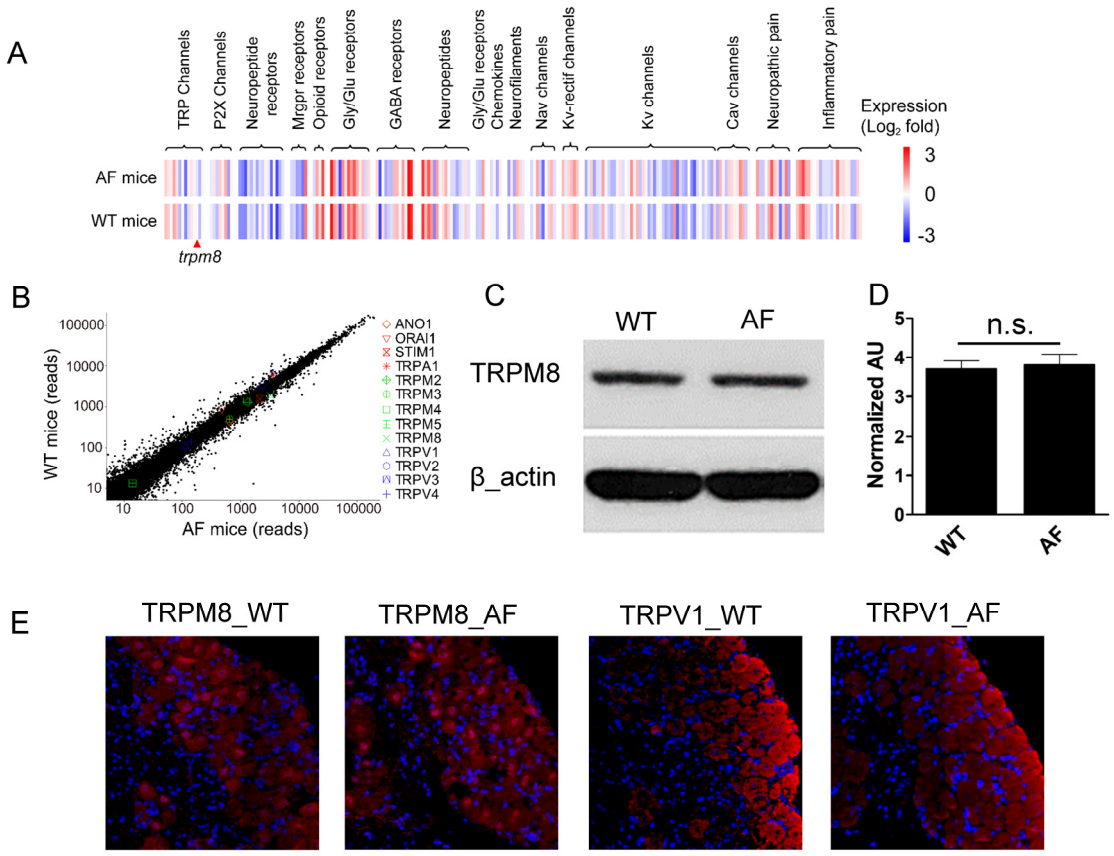


**Fig. S9.** The protein level of TRPM8 in wild-type and AF mice. (A) Heat map showing the differential expression levels in wild type and AF mice of a set of about 200 genes implicated in somatosensation. (B) Transcriptome-wide comparison of mRNA expression between wild-type and AF mice. Several ion channels that have been previously implicated in thermal sensation are indicated. (C) Western blot images of TRPM8 and β-actin in the trigeminal ganglion of wild-type and AF mice. (D) The normalized expression levels of TRPM8 were analyzed in bar graph. (E) Immunostaining of trigeminal ganglia with anti-TRPM8 and anti-TRPV1 antibodies in wild-type and AF mice. Cell nucleuses were stained by DAPI (blue).

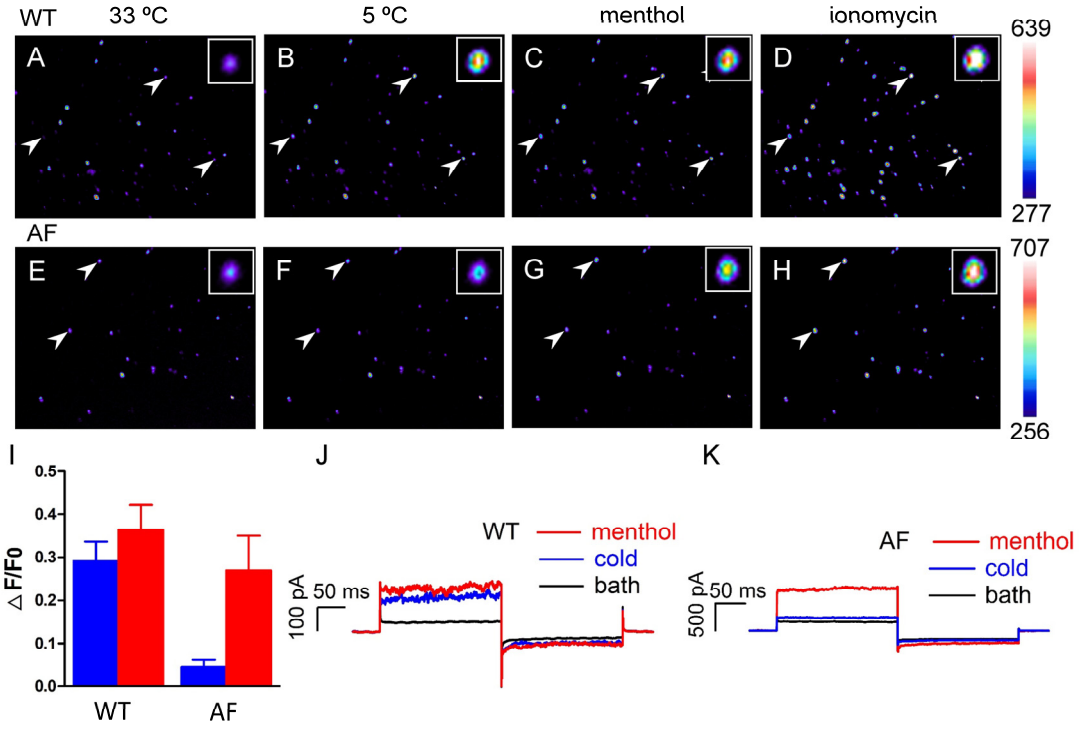


**Fig. S10.** The responses to cold and menthol of DRG neurons. (A-H) Calcium imaging of DRG neurons to cold, 1 mM menthol and 1 mM ionomycin respectively. White arrowheads indicate the cells sequentially challenged with cold and menthol. (I) Average fluorescence change of DRG neurons in response to cold (blue) and 1 mM menthol (red), respectively. (J, K) Representative inside-out patch recordings of DRG neurons in (J) wild-type and (K) AF mice activated by cold and 1 mM menthol.

**Table S1.** Functional comparison of eight vertebrate TRPM8 orthologues.

| Species | Menthol | Cold | Icold/Imenthol |
|---|---|---|---|
| Loxodonta africana | Yes | Yes | 0.843±0.037204 |
| Camelus bactrianus | Yes | Yes | 0.71868±0.03331 |
| Homo sapiens | Yes | Yes | 0.65666±0.04436 |
| Mus musculus | Yes | Yes | 0.6448±0.041383 |
| Jaculus jaculus | Yes | Yes | 0.62782±0.036797 |
| Bos mutus | Yes | Yes | 0.4193±0.039573 |
| Pantholops hodgsonii | Yes | Yes | 0.39548±0.029878 |
| Aptenodytes forsteri | Yes | Yes | 0.14804±0.015487 |

Data shown as mean ± s.e.m. (n=5).

**Table S2.** Functional comparison of TRPM8_AF and TRPM8_LA chimeras.

| Chimeras | The chimeric region | Menthol | Cold | Icold/Imenthol |
|---|---|---|---|---|
| AF | | Yes | Yes | 0.148±0.015 |
| N | 1-691 | No | No | n.d |
| S1 | 688-755 | Yes | Yes | 0.15035±0.0251 |
| S2-S3 | 756-815 | Yes | Yes | 0.285125±0.0250 |
| S4 | 824-852 | No | No | n.d. |
| N-S4 | 1-852 | Yes | Yes | 0.3016±0.0193 |
| S5-S6 | 862-988 | No | No | n.d. |
| S1-S6 | 688-788 | Yes | Yes | 0.778375±0.0393 |
| C | 980-1104 | No | No | n.d. |
| S1-C | 688-1104 | Yes | Yes | 0.702225±0.0248 |
| LA | | Yes | Yes | 0.843±0.037 |

Data shown as means ± s.e.m. (n=4).

**Table S3.** Primers used in this study to generate TRPM8_AF and TRPM8_LA chimeras.

| Chimeras | LA_Primer-Forward | LA_Primer-Reverse | AF_Primer-Forward | AF_Primer-Reverse |
|---|---|---|---|---|
| N | ctggctagcgccaccatgc | aataatcttccagttcttg | tcccgagacaccaagaa | tgcctggaacggcatggtg |
| | cgttccaggcagccaggtt | gtgtctcgggaaatctctc | ctggaagattattttgtgcct | gcgctagccagcttgggtc |
| S1 | Agcagagacacaaagaa | aaagtccatgaggagcacg | Ctgtttgcctacgtgctcc | gataatcttccagttcttt |
| | ctggaagattatcctgtgtct | taggcaaacagcaggagga | tcatggactttcagaagga | gtgtctctgctaatctccc |
| S2-S3 | gtgttcgcctacgtgctg | gctggagtgcaaccgaaa | gcagggattgcatttcggtt | aaaatccatgagcagcacg |
| | ctcatggattttcattcggt | tgcaatccctgctatgaaat | gcactccagcgacgagtc | taggcgaacacgagcagaa |
| S4 | tccagcgacgagtcctct | aatcttaggcccgaggtt | actgtaagcagaaacctc | tccagaatacaaagagga |
| | ttgtattctggacgagtcat | tctgcttacagtgaagatat | gggcctaagattatcatgct | ctcgtcgctggagtgcaacc |
| N-S4 | ctggctagcgccaccatgc | aatcttaggcccgaggtt | actgtaagcagaaacctc | tgcctggaacggcatggtg |
| | cgttccaggcagccaggtt | tctgcttacagtgaagatat | gggcctaagattatcatgct | gcgctagccag cttgggtc |
| S5-S6 | attatcatgctccagagga | cacctgatcgttgttctcct | ggcaccgttcaggagaac | gtcgatcagcatcctctgg |
| | tgctgatcgacgtgttctt | gaacggtgcccaccgtgt | aacgatcaggtgtggaagtt | agcatgataatcttaggcc |
| S1-S6 | tacggggagattagccgag | cacctgatcgttgttctcct | ggcaccgttcaggagaac | gttcttggtgtctcggcta |
| | acaccaagaactggaagat | gaacggtgcccaccgtgt | aacgatcaggtgtggaagtt | atctccccgtaccactgct |
| C | ctggtggccatgtttggcta | gactcgagcggccgctc | aataagatcaaatgagcg | gcccaccgtgtagccaaa |
| | cacggtgggcaccgttca | atttgatcttattagcaatct | gccgctcgagtctagagggc | catggccaccagcaagttca |
| S1-C | tacggggagattagccgag | gactcgagcggccgct | aataagatcaaatgagcg | gttcttggtgtctcggcta |
| | acaccaagaactggaagat | catttgatcttattagcaatct | gccgctcgagtctagagggc | atctccccgtaccactgct |

**Table S4.** Primers used in this study to identify the genotype of AF mice.

| Primer | sequence |
|---|---|
| F1 | 5’-gtggcagcattgaggcatgag-3’ |
| R1 | 5’-tagacaggaaagagagtgactagagg-3’ |

**Table S5.** Routine blood test in wild-type and AF mice.

| Project | WT(n=3) | AF(n=3) |
|---|---|---|
| WBC ($\times 10^9$/L) | 2.85±0.79 | 3.02±0.31 |
| NEUT (%) | 14.83±4.22 | 17.00±0.91 |
| LYM (%) | 81.80±5.90 | 79.77±1.58 |
| NEUT# ($\times 10^9$/L) | 0.36±0.07 | 0.52±0.07 |
| LYM# ($\times 10^9$/L) | 2.42±0.79 | 2.41±0.21 |
| RBC ($\times 10^{12}$/L) | 10.99±0.22 | 11.47±0.28 |
| HGB (g/L) | 158.00±4.93 | 168.33±4.84 |
| HCT (%) | 55.70±0.89 | 59.50±0.76 |
| MCV (fL) | 50.63±0.34 | 51.07±0.12 |
| MCH (pg) | 14.40±0.17 | 14.67±0.09 |
| MCHC (g/L) | 283.67±4.18 | 287.00±2.08 |
| RDW-CV (%) | 21.83±0.35 | 21.73±0.19 |
| RDW-SD (fL) | 25.37±1.15 | 24.77±0.43 |
| PLT ($\times 10^9$/L) | 1188.67±158.62 | 1128.00±91.24 |
| PCT (%) | 0.93±0.09 | 0.86±0.13 |
| MPV (fL) | 7.20±0.15 | 6.97±0.07 |
| PDW (%) | 6.63±1.23 | 7.57±0.12 |
| P-LCR (%) | 6.47±0.84 | 6.70±0.76 |
| NRBC (%) | 0.67±0.44 | 0.50±0.26 |
| NRBC# ($\times 10^9$/L) | 0.01±0.01 | 0.02±0.01 |

Data shown as mean ± s.e.m. (n=3).

**Table S6.** Blood bio-chemistry test in wild-type and AF mice.

| Project | WT(n=3) | AF(n=3) |
|---|---|---|
| TP (g/L) | 58.55±0.26 | 59.53±1.15 |
| ALB (g/L) | 41.78±0.66 | 43.48±2.65 |
| GLB (g/L) | 18.03±0.74 | 17.83±0.62 |
| ALB/GLB | 2.35±0.13 | 2.32±0.20 |
| ALT (IU/L) | 36.83±1.92 | 35.24±0.63 |
| AST (IU/L) | 166.70±2.50 | 175.20±6.97 |
| ALT/AST | 4.23±0.05 | 4.57±0.12 |
| TBIL (μmol/L) | 0.87±0.03 | 1.13±0.03 |
| DBIL (μmol/L) | 0.95±0.18 | 0.77±0.07 |
| IDIL (μmol/L) | 0.40±0.15 | 0.33±0.09 |
| TBA (μmol/L) | 3.60±0.06 | 3.73±0.13 |
| ALP (IU/L) | 126.97±5.55 | 137.30±2.84 |
| UREA (mmol/L) | 11.23±0.61 | 11.88±0.66 |
| CRE (μmol/L) | 19.10±0.22 | 19.90±2.56 |
| UA (μmol/L) | 135.23±2.43 | 138.00±2.08 |
| GLU (mmol/L) | 5.63±0.03 | 5.87±0.20 |
| TCH (mmol/L) | 2.09±0.07 | 2.15±0.03 |
| F-CHOL (mmol/L) | 0.65±0.01 | 0.67±0.03 |

Data shown as mean ± s.e.m. (n=3).

**Video S1.** Representative behavior of wild-type and AF mice when challenged the cold plate during the temperature preference test.

**Dataset S1**. Functional comparison of TRPM8_LA mutants.
**Dataset S2**. Primers used in this study to generate TRPM8_LA mutants.
**Dataset S3**. Functional comparison of ANAP-incorporated TRPM8_LA channels.
**Dataset S4**. Primers used in this study to generate ANAP-incorporated TRPM8_LA channels.
**Dataset S5**. Functional comparison of TRPM8_LA mutants with varying SCH at sites 925, 943 and 947.

**SI References**


1. T. Hessa *et al.*, Recognition of transmembrane helices by the endoplasmic reticulum translocon. *Nature* **433**, 377-381 (2005).
2. C. P. Moon, K. G. Fleming, Side-chain hydrophobicity scale derived from transmembrane protein folding into lipid bilayers. *P Natl Acad Sci USA* **108**, 10174-10177 (2011).
3. A. Leaver-Fay *et al.*, ROSETTA3: an object-oriented software suite for the simulation and design of macromolecules. *Methods Enzymol* **487**, 545-574 (2011).
4. B. Qian *et al.*, High-resolution structure prediction and the crystallographic phase problem. *Nature* **450**, 259-264 (2007).
5. C. Wang, P. Bradley, D. Baker, Protein-protein docking with backbone flexibility. *J Mol Biol* **373**, 503-519 (2007).
6. P. Conway, M. D. Tyka, F. DiMaio, D. E. Konerding, D. Baker, Relaxation of backbone bond geometry improves protein energy landscape modeling. *Protein Sci* **23**, 47-55 (2014).
7. F. Yang *et al.*, The conformational wave in capsaicin activation of transient receptor potential vanilloid 1 ion channel. *Nat Commun* **9**, 2879 (2018).
8. S. J. Fleishman *et al.*, RosettaScripts: a scripting language interface to the Rosetta macromolecular modeling suite. *PLoS One* **6**, e20161 (2011).
9. O. S. Smart, J. M. Goodfellow, B. A. Wallace, The pore dimensions of gramicidin A. *Biophys J* **65**, 2455-2460 (1993).
10. E. F. Pettersen *et al.*, UCSF Chimera--a visualization system for exploratory research and analysis. *J Comput Chem* **25**, 1605-1612 (2004).
11. S. Yang *et al.*, Discovery of a selective NaV1.7 inhibitor from centipede venom with analgesic efficacy exceeding morphine in rodent pain models. *Proceedings of the National Academy of Sciences of the United States of America* **110**, 17534-17539 (2013).